ARMY RESEARCH LABORATORY

Shape Factor of a Randomly Oriented Cylinder

by Richard Saucier

ARL-TR-2269 July 2000

The findings in this report are not to be construed as an official Department of the Army position unless so designated by other authorized documents.

Citation of manufacturer's or trade names does not constitute an official endorsement or approval of the use thereof.

Destroy this report when it is no longer needed. Do not return it to the originator.

Army Research Laboratory
Aberdeen Proving Ground, MD 21005-5068

ARL-TR-2269 **July 2000**

Shape Factor of a Randomly Oriented Cylinder

Richard Saucier
Survivability/Lethality Analysis Directorate, ARL

Abstract

This report defines a dimensionless shape factor, which is useful for characterizing the penetration potential of projectiles and irregular shaped fragments. The shape factor, so defined, is purely a function of shape and orientation and is independent of mass and material density. The shape factor of some simple shapes is calculated exactly, but the focus of this report is on a right circular cylinder (RCC). Not only is it possible to express the shape factor as a function of the length-to-diameter (L/D) ratio and orientation, but it is also possible to derive an exact, closed-form expression for the shape factor probability distribution. It is found that the probability density function is not a symmetrical distribution about its mode, but rather is highly skewed. This points out the inadequacy of an average shape factor and also carries implications for designing fragment simulating projectiles (FSPs). Furthermore, it is shown that randomly oriented cylinders have potential for simulating behind-armor debris fragments.

ACKNOWLEDGMENTS

The author would like to thank Edwin O. Davisson and Linda L. C. Moss for reviewing an earlier version of this report, correcting errors, and suggesting a number of improvements. This report has also benefited substantially from a number of discussions the author had with Robert Shnidman.

INTENTIONALLY LEFT BLANK.

TABLE OF CONTENTS

INTENTIONALLY LEFT BLANK.

LIST OF FIGURES

INTENTIONALLY LEFT BLANK.

LIST OF TABLES

INTENTIONALLY LEFT BLANK.

1. INTRODUCTION

This report defines a dimensionless shape factor, which is useful for characterizing the penetration potential of projectiles and irregular shaped fragments. The shape factor, so defined, is purely a function of shape and orientation and is independent of mass and material density. This is a departure from the past where the previous definition incorporated the material density—so that the shape factor for a steel fragment was different from an aluminum fragment, *even when they had the same size and shape.* Indeed, this fact is easy to overlook with the past definition, and so one can get erroneous results by applying the shape factor for one fragment material to another fragment made from a different material. Past treatments of shape factor have been inadequate in two other respects:

(1) Average shape factor (i.e., the mean value over all orientations) has been used to characterize the entire shape factor distribution over random orientations.

(2) To improve upon the average shape factor, it is common practice to use a normal distribution to simulate an arbitrary orientation.

This report challenges these two assumptions. We show that it is possible to calculate the exact, closed-form expression for the shape factor probability distribution over all orientations of a right circular cylinder with arbitrary length to diameter ratio. This reveals that average shape factor does not do a good job of characterizing an arbitrary orientation, and that the probability distribution is neither normal nor symmetric but rather is skewed in favor of larger shape factors. Since fragment shape factor plays such an important role in penetration and perforation, an improved treatment of shape factor will have important consequences for predictions of fragment perforation and for the design of fragment simulating projectiles (FSPs).

Fragment presented area upon impact with a target plate is a key determinant for penetration, as is fragment mass. Indeed, apart from velocity, the most important factor for penetration is probably the mass per unit presented area. This is borne out by an examination of the THOR penetration equations [1, 2]. The THOR velocity retardation equation is

$$v_r = v_s - k_v (tA)^{\alpha} m_s^{\beta} (\sec\theta)^{\gamma} v_s^{\lambda},$$

where v_r is the residual velocity, v_s is the striking velocity, k_v is a constant, t is the target plate thickness, A is the average presented area of the projectile, m_s is the striking mass, and θ is the obliquity angle. The exponents α and β depend upon the target material. Figure 1 is a plot of these exponents for 20 different target materials, ranging from very soft to very hard.

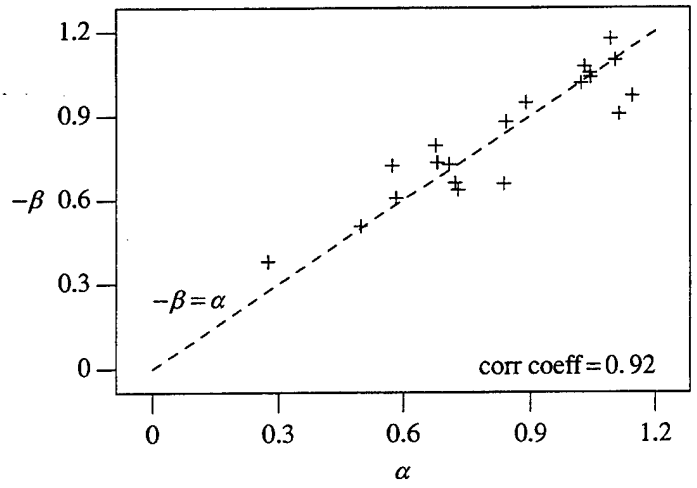

Figure 1. Correlation Between Mass and Presented Area Exponents in THOR Penetration.

It is evident that experimental data support the notion that $-\beta = \alpha$, according to the dashed line—which means that mass and presented area only enter into the THOR penetration equation in the specific combination of m_s/A. Projectile mass is universally recognized as a key parameter for penetration, whereas presented area is perhaps not appreciated to the same extent. But we see here that they are equally important in the THOR penetration equation.

Aside from its volume (which is determined by mass and density), the presented area of a projectile is completely characterized in terms of shape and (except for spheres) orientation. Both of these are contained in the notion of *shape factor*, which we will define momentarily. In this report, we restrict ourselves to the shape of right circular cylinders, for three primary reasons:

(1) Fragment simulating projectiles are usually cylindrical for ease of firing from a gun barrel (as well as the ability to control the impact area through spin-stablization).

(2) Fragment penetration models, such as FATEPEN (Fast Air Target Encounter Penetration) [3], often use cylinders to simulate the fragment shape.

(3) It is simple enough to possess an exact, closed-form expression for the probability density, yet complex enough to have potential for simulating behind-armor debris fragments.

This report focuses on right circular cylinders with arbitrary L/D ratios, where L is the cylinder length and D is the diameter. Also, both specific orientation (e.g., yaw angle) as well as random orientation (uniform over the surface of the unit sphere) are treated.

2. DIMENSIONLESS SHAPE FACTOR

The presented area, A_p, is a function of the dimensions of the cylinder, its shape, and its orientation. The only combination of the mass and material density that has the dimensions of an area is (mass/density)$^{2/3}$. Therefore, the presented area is of the form

$$A_p \equiv \gamma(m/\rho)^{2/3}, \tag{1}$$

where γ is a *dimensionless shape factor* that accounts for both fragment shape and orientation. It is purely a function of geometry and is independent of both mass and density.

Another definition of fragment shape factor that has been used rather extensively is defined by the equation

$$A_p \equiv s\, m^{2/3}. \tag{2}$$

To contrast this with the dimensionless shape factor, we call this quantity s the conventional shape factor. However, this is not a good way to define a shape factor. Aside from the fact that the units are the rather cumbersome $\mathrm{cm}^2/\mathrm{gm}^{2/3}$, or $\mathrm{in}^2/\mathrm{grains}^{2/3}$, the shape factor so defined is dependent upon the material density. Thus, if we determine the shape factor for steel fragments, then they cannot be applied to tungsten fragments *even if they have the same shape* without first accounting for the difference in densities. The dimensionless shape factor defined by equation (1) does not have this restriction. It is easy to convert old values to dimensionless values since the relation between the two is simply

$$\gamma = \begin{cases} \rho^{2/3}\, s & \text{if } s \text{ is in units of } \mathrm{cm}^2/\mathrm{gram}^{2/3} \\ 40\rho^{2/3}\, s & \text{if } s \text{ is in units of } \mathrm{in}^2/\mathrm{grains}^{2/3} \end{cases}, \tag{3}$$

where 1 gram = 15.432 grains. Since the dimensionless shape factor is purely a function of geometry, it is possible to calculate it for various standard shapes, as shown in Table 1.

Table 1. Dimensionless Shape Factors for Some Common Shapes

Shape	*Orientation*	*Shape Factor, γ*
Sphere	Not applicable	$(3/2)^{2/3}(\pi/4)^{1/3} \approx 1.209$
Cube	Face-forward	1
Cube	Edge-forward	$\sqrt{2} \approx 1.414$
Cube	Random[a]	3/2
Cube	Corner-forward	$\sqrt{3} \approx 1.732$
Cylinder (L/D=1)	Face-forward	$(\frac{\pi}{4})^{1/3} \approx 0.927$
Cylinder (L/D=1)	Side-forward	$(\frac{\pi}{4})^{-2/3} \approx 1.175$
Cylinder (L/D=1)	Random[a]	$(3/2)(\pi/4)^{1/3} \approx 1.384$
Artillery Fragment[b]	Random[a]	2.1
Spall Fragment[b]	Random[a]	2.3

a For random orientation, the rule A_p = (Surface Area)/4 was used (see Appendix A).

b The values for artillery and spall fragments were derived from the measured presented area.

In the remainder of this report, we use the terminology "shape factor" to mean the dimensionless shape factor, as defined by equation (1).

3. SHAPE FACTOR OF A CYLINDER

The orientation of the cylinder can be parametrized by the angle θ, as shown in Figure 2.

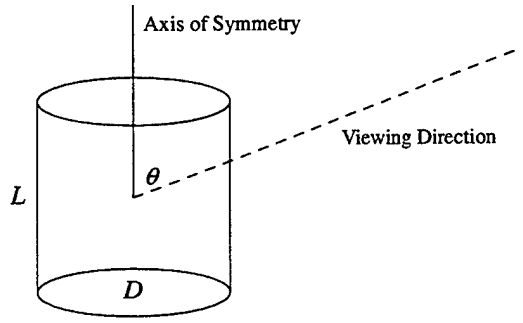

Figure 2. Right Circular Cylinder With Orientation Angle.

When viewed from the side ($\theta = \pi/2$), the projected area is LD. When viewed from the top ($\theta = 0$), the projected area is $\pi D^2/4$. For an arbitrary direction, θ, the projected area is the linear combination of these two faces scaled by the cosine of the projected area surface normal. Thus,

$$A_p = LD\cos(\pi/2 - \theta) + \frac{\pi}{4}D^2|\cos\theta| = D^2\left(\frac{L}{D}\sin\theta + \frac{\pi}{4}|\cos\theta|\right). \tag{4}$$

It is necessary to take the absolute value of the cosine term because $\cos\theta$ is negative when $\pi/2 < \theta \leq \pi$. The volume of the cylinder is given by

$$m/\rho = \frac{\pi}{4}D^2L. \tag{5}$$

Substituting these two expressions into equation (1) and solving for γ, we find that

$$\gamma = \left(\frac{\pi}{4}\frac{L}{D}\right)^{-2/3}\left(\frac{L}{D}\sin\theta + \frac{\pi}{4}|\cos\theta|\right). \tag{6}$$

It is convenient to define the parameters

$$a \equiv \left(\frac{\pi}{4}\frac{L}{D}\right)^{-2/3}\frac{L}{D} \quad \text{and} \quad b \equiv \left(\frac{\pi}{4}\frac{L}{D}\right)^{-2/3}\frac{\pi}{4}. \tag{7}$$

Then the shape factor may be written as

$$\gamma(\theta) = a\sin\theta + b|\cos\theta|, \tag{8}$$

where $0 \le \theta \le \pi$. Notice that the presented area of the cylinder has the same value at the viewing angle θ as it has at $\pi - \theta$, so that $\gamma(\theta) = \gamma(\pi - \theta)$. Thus, we could restrict the orientation to $0 \le \theta \le \pi/2$ and just perform averages over the top hemisphere of the unit sphere. This would allow us to drop the absolute value signs in equation (8). Nevertheless, to avoid confusion, we shall use the form expressed in equation (8) and perform averages over the entire unit sphere.

This expresses the shape factor as an explicit function of the orientation angle, θ. It is also an implicit function of the L/D ratio through the coefficients a and b. A plot of γ as a function of both orientation angle θ and L/D ratio is shown in Figure 3.

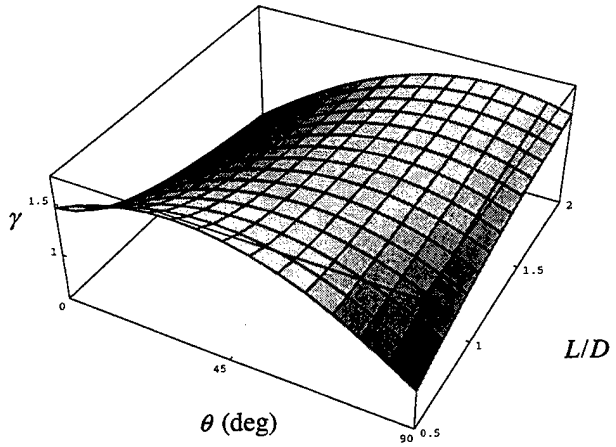

Figure 3. Shape Factor of a Cylinder as a Function of Orientation Angle and L/D Ratio.

From equation (6), we see that $\gamma(0) = b$ and $\gamma(\pi/2) = a$. The *minimum* value of γ is one of these, depending upon the particular L/D ratio:

$$\gamma_{\min} = \begin{cases} a & \text{if } L/D < \pi/4 \\ b & \text{if } L/D > \pi/4 \end{cases} \quad \text{or, simply,} \quad \gamma_{\min} = \min(a, b). \tag{9}$$

The *maximum* value of γ can be obtained by setting $d\gamma/d\theta = 0$, and this gives

$$\gamma_{\max} = \sqrt{a^2 + b^2} = \left(\frac{\pi}{4}\frac{L}{D}\right)^{-2/3}\left[\left(\frac{\pi}{4}\right)^2 + \left(\frac{L}{D}\right)^2\right]^{1/2}. \tag{10}$$

The maximum shape factor is realized at the orientation angle

$$\theta_{\gamma=\gamma_{\max}} = \tan^{-1}\left(\frac{a}{b}\right) = \tan^{-1}\left(\frac{L/D}{\pi/4}\right). \tag{11}$$

Thus, in general, there are two graphs for the shape factor as a function of orientation angle, depending upon the

L/D ratio of the cylinder. These two cases are exemplified in Figures 4 and 5.

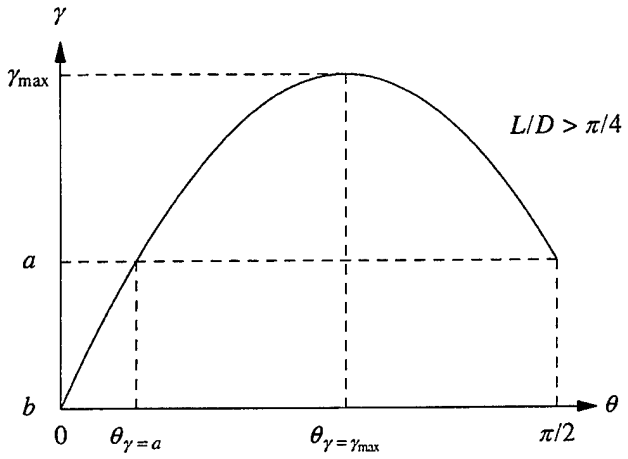

Figure 4. Shape Factor Dependence Upon Orientation for $L/D > \pi/4$.

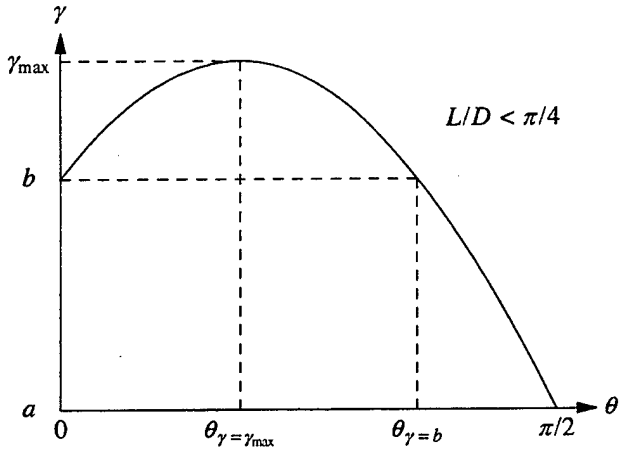

Figure 5. Shape Factor Dependence Upon Orientation for $L/D < \pi/4$.

The angle $\theta_{\gamma=a}$ in Figure 4 and $\theta_{\gamma=b}$ in Figure 5 can be obtained through the use of equation (8) and we find

$$\theta_{\gamma=a} = \tan^{-1}\left(\frac{a^2 - b^2}{2ab}\right) \quad \text{when} \quad L/D > \pi/4 \tag{12}$$

and

$$\theta_{\gamma=b} = \tan^{-1}\left(\frac{2ab}{b^2 - a^2}\right) \quad \text{when} \quad L/D < \pi/4. \tag{13}$$

From Figures 4 and 5, we also see that when $\max(a, b) \leq \gamma \leq \gamma_{\max}$, the orientation angle is double-valued, and when $\min(a, b) \leq \gamma < \max(a, b)$, the orientation angle is single-valued.

4. SHAPE FACTOR AS A FUNCTION OF ORIENTATION

The minimum shape factor is given by equation (9), and the maximum shape factor is given by equation (10). The mean shape factor, when averaged over all orientations equally, is given by

$$\bar{\gamma} = \frac{1}{4\pi}\int \gamma(\theta)d\Omega = \frac{1}{4\pi}\int_0^{2\pi} d\phi \int_0^{\pi} \gamma(\theta)\sin\theta d\theta. \tag{14}$$

Substituting equation (8) and performing the integration, we find†

$$\bar{\gamma} = a\frac{\pi}{4} + b\frac{1}{2} = \left(\frac{\pi}{4}\right)^{1/3}\left(\frac{L}{D}\right)^{-2/3}\left(\frac{L}{D}+\frac{1}{2}\right). \tag{15}$$

Calculation shows that $\bar{\gamma}$ is a minimum when $L/D = 1$, where it takes on the value $(3/2)(\pi/4)^{1/3} \approx 1.38395$. If we only know the average shape factor of a fragment, and it exceeds this value, then eq. (15) can be used to find the L/D ratio of an equivalent disk-shaped cylinder. This solution is shown plotted in Figure 6.

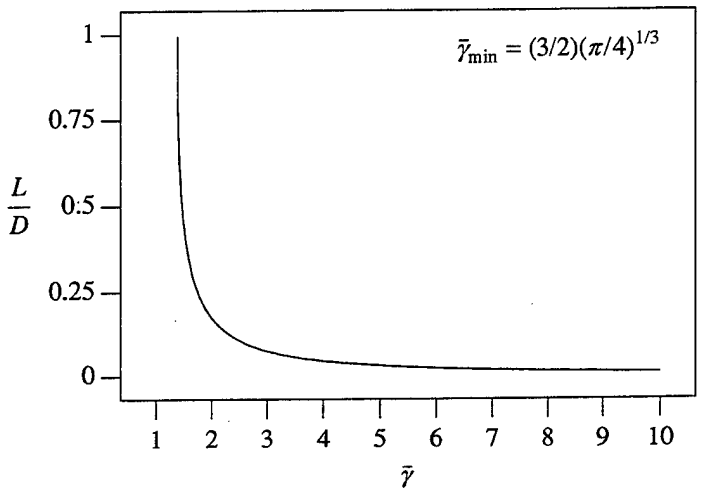

Figure 6. Disk-Shaped Cylinder Derived From the Average Shape Factor.

Here is a simple program that implements this solution of the cubic equation for the L/D ratio:

```
// asf2ld.C: Find the L/D ratio of an RCC with the given average shape factor.

#include <iostream.h>
#include <math.h>

void main( void )
{
   const double C         = pow( 0.25 * M_PI, -1. / 3. );
   const double G_BAR_MIN = 1.5 / C;

   double l_dMin, gBar;

   while ( cin >> gBar ) {

      if ( gBar > G_BAR_MIN ) {
         double p = sqrt( 2. * C * gBar / 3. );
         double q = acos( -pow( p, -3. ) );
         l_dMin = pow( 2. * p * cos( q / 3. ), -3. );
      }
      else if ( gBar == G_BAR_MIN ) l_dMin = 1.;
      else {
         cerr << "The minimum average shape factor for an RCC is "
              << G_BAR_MIN << endl;
         exit( 1 );
      }
      cout << l_dMin << endl;
   }
}
```

† This result also follows from the general theorem that the average projected area of a convex solid is one-fourth the total surface area (see Appendix A).

The average, minimum, and maximum shape factors are plotted in Figure 7.

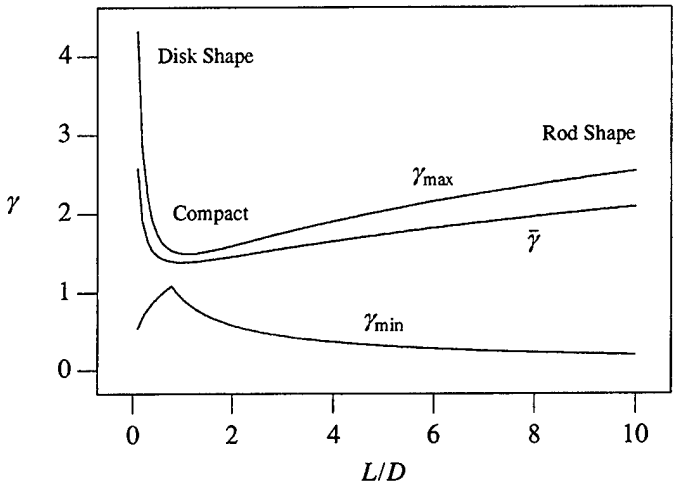

Figure 7. Minimum, Maximum, and Mean Shape Factors as a Function of L/D Ratio.

It is straightforward to establish the following:

- $\bar{\gamma}$ is a minimum when $L/D = 1$.
- γ_{max} is a minimum when $L/D = \sqrt{2}\,\pi/4 \approx 1.111$.
- γ_{min} is a maximum when $L/D = \pi/4 \approx 0.785$.
- $\gamma_{max} - \gamma_{min}$ (i.e., the range of γ over all possible orientations) is a minimum when $L/D = \pi/4 \approx 0.785$. Its value at the minimum is $(\sqrt{2}-1)(\pi/4)^{-1/3} \approx 0.449$. This quantity is a measure of the deviation from spherical symmetry, since a sphere has $\gamma_{max} - \gamma_{min} = 0$.

For completeness, we can also calculate the variance:

$$\sigma^2 = \frac{1}{4\pi}\int(\gamma(\theta)-\bar{\gamma})^2 d\Omega = \int_0^{\pi/2}(\gamma(\theta)-\bar{\gamma})^2 \sin\theta\, d\theta, \tag{16}$$

and we find

$$\sigma^2 = \left(\frac{2}{3}-\frac{\pi^2}{16}\right)a^2 + \left(\frac{2}{3}-\frac{\pi}{4}\right)ab + \frac{1}{12}b^2. \tag{17}$$

5. SHAPE FACTOR DISTRIBUTION OF A RANDOMLY ORIENTED CYLINDER

It is possible to derive a closed-form expression for the shape factor probability distribution function. We start with the formula for the probability density.

$$f(\gamma) = \int_0^{\pi/2} \delta(a\sin\theta + b\cos\theta - \gamma)\sin\theta\, d\theta, \tag{18}$$

where $\delta(x)$ is the Dirac delta function, or, setting $x = \cos\theta$,

$$f(\gamma) = \int_0^1 \delta(g(x))\, dx, \tag{19}$$

where

$$g(x) \equiv a\sqrt{1-x^2} + bx - \gamma. \tag{20}$$

To evaluate this integral, we use the fact that the delta function *of a function* can be expressed in terms of the roots of

the function [4]:

$$\delta(g(x)) = \sum_{i=1}^{n} \frac{\delta(x - x_i)}{|\, dg/dx \,|_{x=x_i}}, \tag{21}$$

where x_i $(i = 1, \cdots, n)$ are the n roots of the equation $g(x) = 0$. The roots of $g(x)$ are found to be

$$x = \frac{b\gamma \pm a\sqrt{a^2 + b^2 - \gamma^2}}{a^2 + b^2}. \tag{22}$$

This can be simplified by introducing the quantities

$$a' \equiv \frac{a}{\gamma_{\max}}, \quad b' \equiv \frac{b}{\gamma_{\max}}, \quad \text{and} \quad \gamma' \equiv \frac{\gamma}{\gamma_{\max}}, \tag{23}$$

where $\gamma_{\max}$ is given by eq. (10). The roots can now be written as

$$x = b'\gamma' \pm a'\sqrt{1 - \gamma'^2}. \tag{24}$$

Now notice that $a'^2 + b'^2 = 1$ and $0 < \gamma' \leq 1$ so that we can define angles

$$\alpha \equiv \cos^{-1}(b') = \cos^{-1}(b/\gamma_{\max}) \quad \text{and} \quad \beta \equiv \cos^{-1}(\gamma') = \cos^{-1}(\gamma/\gamma_{\max}). \tag{25}$$

This allows us to express eq. (24) as

$$x = \cos\alpha \cos\beta \pm \sin\alpha \sin\beta = \cos(\alpha \pm \beta). \tag{26}$$

So the two roots are

$$x_1 = \cos(\alpha - \beta) \quad \text{and} \quad x_2 = \cos(\alpha + \beta), \tag{27}$$

or, in terms of the orientation angle, θ,

$$\theta_1 = \alpha - \beta \quad \text{and} \quad \theta_2 = \alpha + \beta. \tag{28}$$

Evaluation of the derivative of $g(x)$ is straightforward, and we find

$$g'(x_1) = \frac{\gamma_{\max} \sin(-\beta)}{\sin(\alpha - \beta)} \quad \text{and} \quad g'(x_2) = \frac{\gamma_{\max} \sin\beta}{\sin(\alpha + \beta)}. \tag{29}$$

Thus,

$$f(\gamma) = \int_0^1 \delta(g(x))dx = \int_0^1 \left(\frac{\delta(x - x_1)}{|g'(x_1)|} + \frac{\delta(x - x_2)}{|g'(x_2)|} \right) dx, \tag{30}$$

and, using equation (29),

$$f(\gamma) = \int_0^1 \left(\frac{|\sin(\alpha - \beta)|}{|\gamma_{\max} \sin(-\beta)|} \delta(x - x_1) + \frac{|\sin(\alpha + \beta)|}{|\gamma_{\max} \sin(\beta)|} \delta(x - x_2) \right). \tag{31}$$

In order to evaluate this integral, it is sufficient to know the location of the two roots, x_1 and x_2, or, equivalently, θ_1 and θ_2. For $L/D > \pi/4$, we find that when $b \leq \gamma < a$, then $0 \leq \theta_1 < \theta_{\gamma=a}$ and when $a \leq \gamma \leq \gamma_{\max}$, then $\theta_1 = \theta_{\gamma=a}$ and $\theta_{\gamma=\gamma_{\max}} \leq \theta_2 \leq \pi/2$. Similarly, when $L/D < \pi/4$, we find that when $a \leq \gamma < b$, then $\theta_{\gamma=b} < \theta_2 \leq \pi/2$ and when $b \leq \gamma \leq \gamma_{\max}$, then $0 \leq \theta_1 \leq \theta_{\gamma=\gamma_{\max}}$ and $\theta_2 = \theta_{\gamma=b}$. Thus, only one root lies in the interval where the orientation angle is single-valued and both roots lie in the interval where the orientation angle is double-valued. The evaluation of the integral is now trivial, and the results are as follows.

- **$L/D > \pi/4$**

$$\text{If } b \leq \gamma < a, \text{ then } f(\gamma) = \frac{\sin(\alpha - \beta)}{\gamma_{\max} \sin\beta}. \tag{32}$$

$$\text{If } a \leq \gamma < \gamma_{\max}, \text{ then } f(\gamma) = \frac{\sin(\alpha - \beta)}{\gamma_{\max} \sin\beta} + \frac{\sin(\alpha + \beta)}{\gamma_{\max} \sin\beta}. \tag{33}$$

- ***L / D < π / 4***

$$\text{If } a \le \gamma < b, \text{ then } f(\gamma) = \frac{\sin(\alpha + \beta)}{\gamma_{max} \sin \beta}. \tag{34}$$

$$\text{If } b \le \gamma < \gamma_{max}, \text{ then } f(\gamma) = \frac{\sin(\alpha - \beta)}{\gamma_{max} \sin \beta} + \frac{\sin(\alpha + \beta)}{\gamma_{max} \sin \beta}. \tag{35}$$

Expressing these results in terms of the parameters a and b gives us the following results.

5.1 Probability Density Function

- ***L / D > π / 4***

$$f(\gamma) = \begin{cases} \dfrac{a\gamma - b\sqrt{\gamma_{max}^2 - \gamma^2}}{\gamma_{max}^2 \sqrt{\gamma_{max}^2 - \gamma^2}} & b \le \gamma < a \quad 0 \le \theta < \theta_d \\ \dfrac{2a\gamma}{\gamma_{max}^2 \sqrt{\gamma_{max}^2 - \gamma^2}} & a \le \gamma < \gamma_{max} \quad \theta_d \le \theta < \pi/2 \end{cases} \tag{36}$$

Figure 8 is a plot of this function for a compact cylinder.

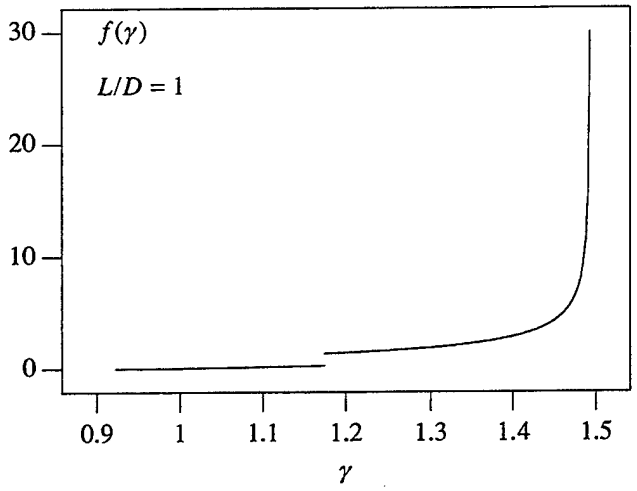

Figure 8. Shape Factor Probability Density Function for a Cylinder With $L/D > \pi/4$.

Notice the discontinuity at $\gamma = (\pi/4)^{-2/3}$, where the shape factor changes from being single-valued to being double-valued.

- ***L / D < π / 4***

$$f(\gamma) = \begin{cases} \dfrac{a\gamma + b\sqrt{\gamma_{max}^2 - \gamma^2}}{\gamma_{max}^2 \sqrt{\gamma_{max}^2 - \gamma^2}} & a \le \gamma < b \quad \theta_d < \theta < \pi/2 \\ \dfrac{2a\gamma}{\gamma_{max}^2 \sqrt{\gamma_{max}^2 - \gamma^2}} & b \le \gamma \le \gamma_{max} \quad 0 \le \theta \le \theta_d \end{cases} \tag{37}$$

Figure 9 shows a plot of these functions for a disk-shaped cylinder.

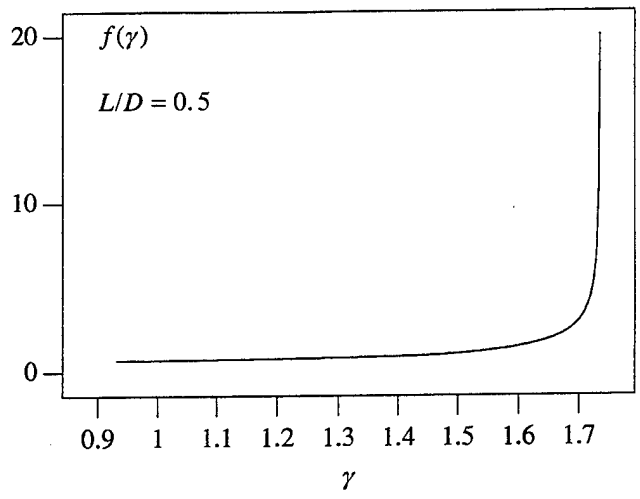

Figure 9. Shape Factor Probability Density Function for a Cylinder with $L/D < \pi/4$.

Notice that the most probable value of the shape factor, (i.e., its *mode*), is γ_{max}, regardless of the magnitude of the L/D ratio.

5.2 Cumulative Distribution Function

- ***L/D > π / 4***

$$F(\gamma) = \begin{cases} 1 - \dfrac{b\gamma + a\sqrt{\gamma_{max}^2 - \gamma^2}}{\gamma_{max}^2} & b \le \gamma < a \quad 0 \le \theta < \theta_d \\ 1 - \dfrac{2a\sqrt{\gamma_{max}^2 - \gamma^2}}{\gamma_{max}^2} & a \le \gamma \le \gamma_{max} \quad \theta_d \le \theta \le \pi/2 \end{cases} \tag{38}$$

Figure 10 is a plot of the cumulative distribution for a compact cylinder.

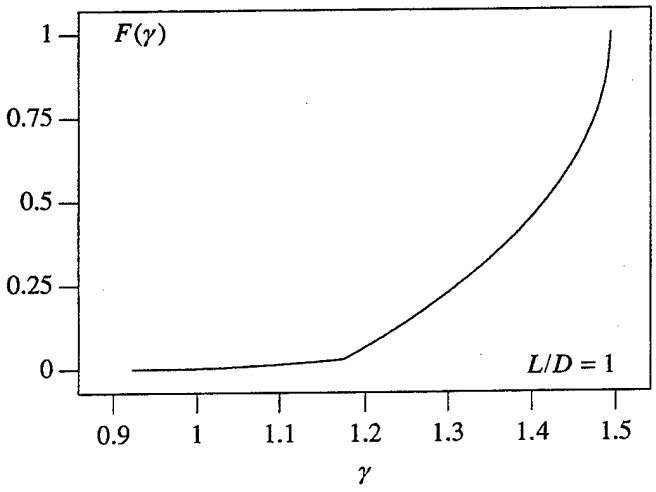

Figure 10. Shape Factor Cumulative Distribution Function for a Cylinder With $L/D > \pi/4$.

- ***Case: L/D < π / 4***

$$F(\gamma) = \begin{cases} \dfrac{b\gamma - a\sqrt{\gamma_{max}^2 - \gamma^2}}{\gamma_{max}^2} & a \le \gamma < b \quad \theta_d \le \theta < \pi/2 \\ 1 - \dfrac{2a\sqrt{\gamma_{max}^2 - \gamma^2}}{\gamma_{max}^2} & b \le \gamma \le \gamma_{max} \quad 0 \le \theta \le \theta_d \end{cases} \tag{39}$$

A plot of this cumulative distribution for a disk-shaped cylinder is shown in Figure 11.

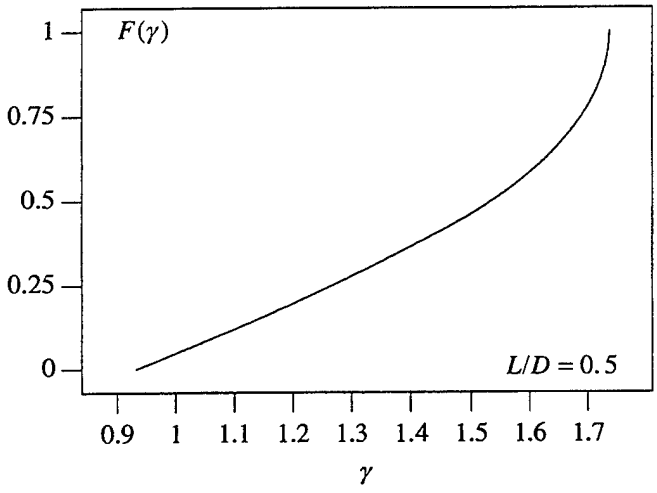

Figure 11. Shape Factor Cumulative Distribution Function for a Cylinder With $L/D < \pi/4$.

5.3 Generating the Random Shape Factor Distribution

The cumulative distribution expressed by equations (38) and (39) can be inverted to give γ in terms of the cumulative probability. Then by selecting the cumulative probability from a uniform random distribution on the unit interval, we generate a random distribution of shape factors, where the frequency of occurrence follows the probability density function—a standard technique for generating random numbers.

- ***Case: L/D > π / 4***

$$\gamma = \begin{cases} b(1-P) + a\sqrt{1-(1-P)^2} & 0 \le P \le 1 - 2ab/\gamma_{max}^2 \\ \gamma_{max}\sqrt{1-(\gamma_{max}(1-P)/2a)^2} & 1 - 2ab/\gamma_{max}^2 \le P \le 1 \end{cases} \tag{40}$$

- ***Case: L/D < π / 4***

$$\gamma = \begin{cases} bP + a\sqrt{1-P^2} & 0 \le P \le (b^2 - a^2)/\gamma_{max}^2 \\ \gamma_{max}\sqrt{1-(\gamma_{max}(1-P)/2a)^2} & (b^2 - a^2)/\gamma_{max}^2 \le P \le 1 \end{cases} \tag{41}$$

These equations enable us to define an algorithm for generating random shape factors having the same distribution as that corresponding to the uniform random orientation of a cylinder. First, define the following quantities:

$$a \equiv \left(\frac{\pi}{4}\frac{L}{D}\right)^{-2/3}\frac{L}{D}, \quad b \equiv \left(\frac{\pi}{4}\frac{L}{D}\right)^{-2/3}\frac{\pi}{4}, \quad \gamma_{\max} = \sqrt{a^2+b^2}, \quad P_1 \equiv 1 - \frac{2ab}{\gamma_{\max}^2}, \quad \text{and} \quad P_2 \equiv \frac{(b^2-a^2)}{\gamma_{\max}^2}.$$

Then the algorithm is:

(1) Generate $P \sim U(0,1)$.
(2) If $a \geq b$, (i.e, $L/D \geq \pi/4$),
  (2a) If $P \leq P_1$, return $\gamma = b(1-P) + a\sqrt{1-(1-P)^2}$.
  (2b) Else if $P > P_1$, return $\gamma = \gamma_{\max}\sqrt{1-(\gamma_{\max}(1-P)/2a)^2}$.
(3) Else if $a < b$, (i.e, $L/D < \pi/4$),
  (3a) If $P \leq P_2$, return $\gamma = bP + a\sqrt{1-P^2}$.
  (3b) Else if $P > P_2$, return $\gamma = \gamma_{\max}\sqrt{1-(\gamma_{\max}(1-P)/2a)^2}$.

This algorithm is more than twice as fast in execution time than the considerably simpler shape factor *simulation*:

(1) Generate $(\theta, \phi) \sim$ Surface of the Unit Sphere.†
(2) Return $\gamma = a\sin\theta + b\cos\theta$.

Before moving on, we summarize some properties of the shape factor distribution for a randomly oriented cylinder in Table 2.

Table 2. Shape Factor Parameters for a Randomly Oriented Cylinder

Parameter	*Expression*	*Values when L/D = 1*
Length	L	L
Diameter	D	L
Parameter a	$a = \left(\frac{\pi}{4}\frac{L}{D}\right)^{-2/3}\frac{L}{D}$	$a = 1.17474$
Parameter b	$b = \left(\frac{\pi}{4}\frac{L}{D}\right)^{-2/3}\frac{\pi}{4}$	$b = 0.922635$
Minimum	$\gamma_{\min} = \min(a,b)$	$\gamma_{\min} = 0.922635$
Maximum	$\gamma_{\max} = \sqrt{a^2+b^2}$	$\gamma_{\max} = 1.49374$
Mean	$\bar{\gamma} = \frac{\pi}{4}a + \frac{1}{2}b$	$\bar{\gamma} = 1.38395$
Variance	$\sigma^2 = \left(\frac{2}{3} - \frac{\pi^2}{16}\right)a^2 + \left(\frac{2}{3} - \frac{\pi}{4}\right)ab + \frac{1}{12}b^2$	$\sigma^2 = 0.0109974$
Mode	$\hat{\gamma} = \gamma_{\max}$	$\hat{\gamma} = 1.49374$
Median	$\tilde{\gamma} = \begin{cases} \gamma_{\max}\sqrt{1-(\gamma_{\max}/4a)^2} & \text{if } \frac{\pi}{4} < \frac{L}{D} < (\sqrt{3}+2)\frac{\pi}{4} \\ \frac{\sqrt{3}a+b}{2} & \text{if } (\sqrt{3}+2)\frac{\pi}{4} < \frac{L}{D} \\ \gamma_{\max}\sqrt{1-(\gamma_{\max}/4a)^2} & \text{if } \frac{1}{\sqrt{3}}\frac{\pi}{4} < \frac{L}{D} < \frac{\pi}{4} \\ \frac{\sqrt{3}a+b}{2} & \text{if } \frac{L}{D} < \frac{1}{\sqrt{3}}\frac{\pi}{4} \end{cases}$	$\tilde{\gamma} = 1.41626$

† See Saucier [5] for an algorithm to generate angle pairs (θ, ϕ) that lie on the surface of the unit sphere.

6. SIMULATION OF BEHIND-ARMOR DEBRIS FRAGMENTS

As the L/D ratio decreases, and the fragment becomes more disk-like, the probability density function $f(\gamma)$ becomes nearly constant everywhere except very close to γ_{max}, where it becomes highly peaked. Consequently, the cumulative distribution function $F(\gamma)$ becomes almost a straight line over nearly its entire domain. For example, Figure 12 shows a plot of the $F(\gamma)$ for an L/D of 0.1.

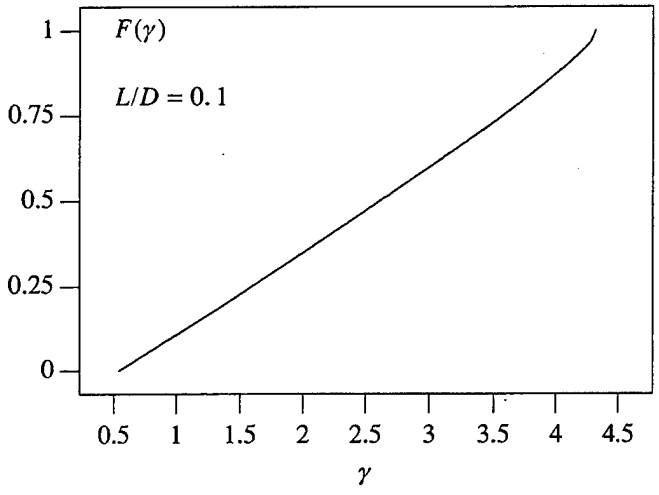

Figure 12. Shape Factor Cumulative Distribution Function for a Cylinder With Small L/D.

Thus, if fragments can be simulated with small–L/D–ratio, disk-shaped cylinders, then we should expect a relatively flat, or uniform, shape factor distribution over orientation angle. While this pertains to a single fragment, what about a distribution of fragments? Since there is no obvious reason why the fragments would be expected to have all the same L/D ratio, let us assume that they vary over some finite range. How will this affect the shape factor distribution? For example, Figure 13 shows four cylinders with different L/D ratios. As a point of reference, a dime has an L/D of 0.1.

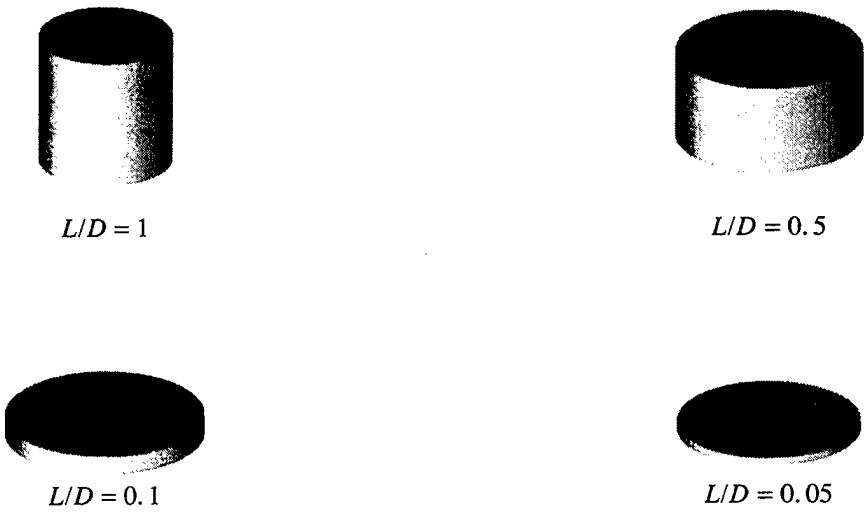

Figure 13. Four Cylinders of the Same Mass but Different L/D Ratios.

Let us assume that the L/D ratio is equally likely to be anywhere from 0.05 to 0.5, and that each fragment is oriented uniformly over the unit sphere. To determine the resultant shape factor distribution, we perform a Monte Carlo simulation. Figure 14 shows a typical result.

```
Midpt     Freq
0.109        0
0.326        0
0.543        0
0.761       11 ***********
0.978       23 ***********************
1.195       35 ***********************************
1.413       41 *****************************************
1.630       54 ******************************************************
1.847       40 ****************************************
2.065       25 *************************
2.282       17 *****************
2.499       14 **************
2.717        6 ******
2.934        9 *********
3.151        9 *********
3.369        5 *****
3.586        1 *
3.803        3 ***
4.021        1 *
4.238        1 *
4.455        2 **
4.672        0
4.890        2 **
5.107        0
5.324        1 *
```

Figure 14. Shape Factor Simulation from Randomly Oriented Cylinders With Uniformly Distributed L/D Ratios.

The distribution appears to be lognormal. In any case, it is skewed to larger shape factors, and is far from uniform. In summary:

- A fragment in the shape of a disk-like cylinder with a small but fixed L/D ratio leads to a uniform distribution of shape factors.
- A collection of fragments in the shape of disk-like cylinders with small but varying L/D ratios leads to a distribution of shape factors that is skewed to larger values and appears to be lognormal.

The next step is to compare these results to experimental data.

6.1 Experimental Design to Collect Behind-Armor Debris

Behind-armor debris fragments were collected in Cellotex when a 30–mm armor piercing discarding sabot (APDS) round was shot at a 1–inch–thick target of rolled homogeneous armor (RHA). The debris fragments were subsequently collected and weighed. Then each fragment was placed in a device that measures the presented area from 16 different orientation angles.† Knowing the mass of the fragment and its presented area allows us to derive a value of the shape factor by making use of equation (1).

6.2 Analysis of Shape Factor Data

Figure 15 shows the shape factor distribution for one of the spall fragments, as measured from 16 viewing angles.

† The firings and fragment collection were performed by Robert F. Kinsler at the U.S. Army Research Laboratory Experimental facility. The measurements of the fragment presented area from 16 different viewpoints were performed at the U.S. Army Aberdeen Test Center.

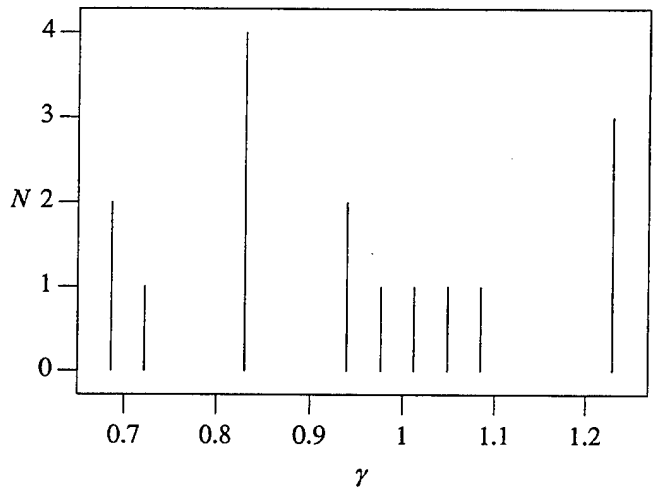

Figure 15. Shape Factor of a Spall Fragment from 16 Viewing Directions.

Although the frequency distribution shows scatter, the shape factor is relatively uniform over orientation angle. Since 16 viewpoints are not very many, we should expect a certain amount of variation. For example, Figure 16 shows the shape factor simulation results from viewing a randomly oriented cylinder with an $L/D = 0.1$.

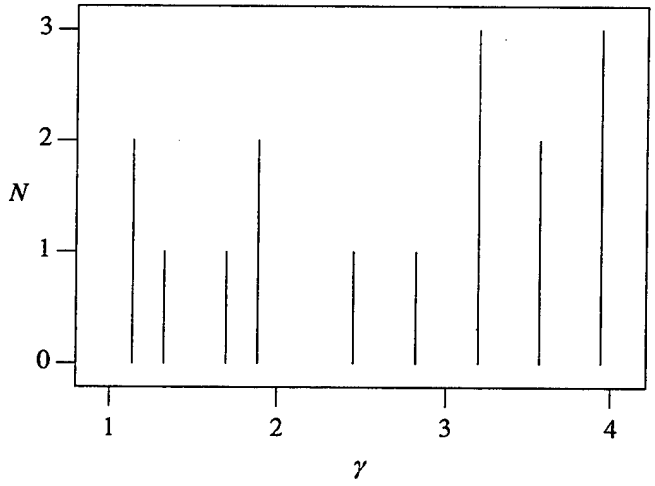

Figure 16. Simulation of Shape Factor Distribution from 16 Viewing Directions.

In this particular shot, 150 spall fragments were recovered. They ranged in mass from 0.02 grains to several hundred grains (where the larger masses may very well be broken pieces of the penetrator). The fragment masses appear to be lognormally distributed.† Now we might expect there to be a correlation between the mass of a fragment and its shape factor distribution. For example, one might expect a smaller fragment to be more compact, like a sphere, and a larger fragment to be more irregular in shape. The first question to address, then, is whether there is a systematic trend between the mass of the fragment and its shape. To test this, we compute the linear correlation coefficient. The correlation coefficient between two variables x and y is defined by

$$r = \frac{\mathrm{cov}\,(x, y)}{\sigma_x \sigma_y}, \tag{42}$$

† The behind-armor debris mass distribution is commonly fitted with a Weibull distribution, where it goes by the name of Rosin-Rammler distribution. We have found, however, that a lognormal gives a better fit to this data.

where

$$\mathrm{cov}\,(x, y) \equiv \frac{1}{n-1}\sum_{i=1}^{n}(x_i - \bar{x})(y_i - \bar{y}) \tag{43}$$

is the sample covariance of the n (x, y) data pairs and

$$\sigma_x^2 \equiv \frac{1}{n-1}\sum_{i=1}^{n}(x_i - \bar{x})^2 \tag{44}$$

is the sample variance. The value for r always lies in the range $[-1, 1]$, with a value of 0 indicating the variables are uncorrelated. For a nonzero value *close* to zero, we use the fact that the test statistic

$$t = \frac{r\sqrt{n-2}}{\sqrt{1-r^2}} \tag{45}$$

is distributed according to Student's distribution and use it to test the null hypothesis that the actual correlation coefficient is zero,

$$H_0\colon \rho = 0, \tag{46}$$

where ρ is the actual correlation coefficient. The computed correlation coefficient between the mass of the fragment and the average shape factor is found to be $r = -0.130$. Our test statistic is $t = -1.60$. From a table of Student's distribution, we find that this is smaller (in absolute value) than 1.96, the critical value for a two-sided test at the 0.05 level of significance. This means we cannot reject the hypothesis that these two variables are uncorrelated. Another indicator of compactness, or lack thereof, is the difference between the maximum and minimum shape factors. The correlation coefficient between this difference and mass is found to be $r = -0.076$. The test statistic is $t = -0.93$. Once again, since this is smaller than 1.96 in absolute value, we cannot reject the hypothesis that these two variables are uncorrelated. These tests show that there does not appear to be any statistical correlation between shape factor and mass. Therefore, we do not introduce any systematic bias by pooling all the shape factors regardless of mass. This gives us a total of 2,400 shape factors (i.e., 16 views × 150 masses) from which to determine the shape factor distribution. This is shown plotted as a histogram in Figure 17.

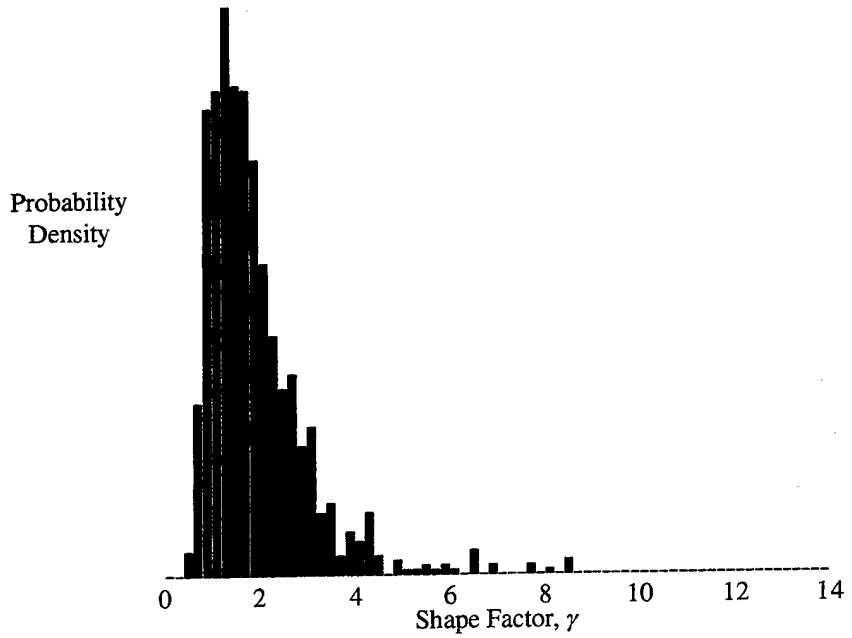

Figure 17. Empirical Shape Factor Probability Distribution.

The empirical distribution appears to be lognormal—and resembles very much the distribution obtained by varying the L/D ratio of disk-like cylinders (cf. Figure 13).

6.3 Monte Carlo Simulation of Shape Factor

Thus, it appears that randomly oriented, disk-like cylinders have the potential for simulating real behind-armor debris fragments. This is about as far as we can go without additional experiments. The experiments cited in this report do not attempt to classify fragments as either spall, originating from the RHA target, or broken pieces of the penetrator. The penetrator in this case was made of tungsten with a material density of 17.6 gm/cm^3. If γ_{St} denotes the fragment shape factor computed assuming that the material was steel, and the fragment was actually composed of tungsten, then the correct shape factor is

$$\gamma_W = \gamma_{St}\,(17.6/7.8)^{2/3} = 1.72\,\gamma_{St}. \tag{47}$$

So this can have a significant effect upon the shape factor distribution. Indeed, at face value, we cannot obtain an L/D ratio for all of the empirical data, due to the fact that the smallest average shape factor for a cylinder is 1.3895. The smallest average shape factor from the empirical data is 0.8424. Notice, however, that if this is actually a tungsten fragment, then the average shape factor is $1.72 \times 0.8424 = 1.4489$, which does lie within the range of a cylindrical shape.

A procedure for using disk-like cylinders to simulate behind-armor debris fragments can be formulated as follows:

- Collect behind-armor debris fragments and identify the material density.
- Use equation (15) to compute the L/D ratio from the average shape factor.
- Identify a probability density function that captures the L/D distribution. Denote this distribution by $F(L/D)$; the simulation leading to Figure 13 assumed that this was the Uniform distribution.

Once the $F(L/D)$ distribution is known, an algorithm for a Monte Carlo simulation is as follows:

(1) Generate $L/D \sim F(L/D)$.
(2) Generate $(\theta, \phi) \sim$ Surface of the Unit Sphere.
(3) Return $\gamma = a \sin\theta + b \cos\theta$, where a and b are given by equation (7).

Once the mass m, density ρ, and L/D ratio of the fragment are known, then the actual dimensions of the fragment can be computed:

$$D = \left(\frac{m/\rho}{(\pi/4)(L/D)}\right)^{1/3} \quad \text{and} \quad L = \left(\frac{L}{D}\right)D. \tag{48}$$

7. CONCLUSIONS

A dimensionless shape factor was defined and applied to a randomly oriented right circular cylinder. This analysis established the following results.

- The L/D ratio of a disk-shaped cylinder can be obtained from the average shape factor (see p. 6).
- An explicit probability density function can be obtained for a randomly oriented cylinder.
- Two algorithms can be used for simulating randomly oriented cylinders:
  - A fast method, derived from the inverse transformation technique.
  - An explicit simulation of the oriented cylinder.
- Shape factors for disk-shaped cylinders show potential for simulating behind-armor debris fragments.

It should also be noted that the average shape factor should not be used in place of the shape factor distribution. For example, consider a 1–gm steel cylinder with an $L/D = 0.1$ striking a 1/32–inch mild steel plate at a speed of 360 m/s. The THOR penetration equations indicate that the projectile will perforate the plate only if $\gamma \le 2.3$. Since the average shape factor for this L/D ratio is 2.6, using $\bar{\gamma}$ to represent the projectile, will lead to the conclusion that there is no perforation. Using the shape factor distribution, however, shows that there is indeed perforation in 42% of the impact encounters due to the effect of random orientation (cf. Figure 12).

The results derived in this report should be used for designing fragment–simulating projectiles. And since the FATEPEN code explicitly models penetrators as right circular cylinders, fully accounting for both orientation and L/D ratio, these results should also be useful when using that model for simulating fragment penetration.

INTENTIONALLY LEFT BLANK.

8. REFERENCES

[1] Project THOR. "The Resistance of Various Metallic Materials to Perforation by Steel Fragments; Empirical Relationships for Fragment Residual Velocity and Residual Weight." TR-47, U.S. Army Ballistic Analysis Laboratory, Institute for Cooperative Research, The Johns Hopkins University, April 1961.

[2] Project THOR. "The Resistance of Various Non-Metallic Materials to Perforation by Steel Fragments; Empirical Relationships for Fragment Residual Velocity and Residual Weight." TR-51, U.S. Army Ballistic Analysis Laboratory, Institute for Cooperative Research, The Johns Hopkins University, April 1963.

[3] Zernow, Richard H., Kellye C. Frew, and Jerome Yatteau. "FATEPEN2 in MUVES Software Design Document," Contract #DAAA15-94-D-0005 Delivery Order 0003, ARA Project 5948, Applied Research Associates, Inc., Littleton, CO, and Albuquerque, NM, April 26, 1995.

[4] Dennery, Philippe, and Andre Krzywicki. *Mathematics for Physicists*. New York: Harper & Row, 1967.

[5] Saucier, Richard. "Computer Generation of Statistical Distributions," Technical report, U.S. Army Research Laboratory, Aberdeen Proving Ground, MD, to be published.

INTENTIONALLY LEFT BLANK.

APPENDIX A:
MEAN PRESENTED AREA OF A CONVEX SOLID

Let $\mathbf{n}$ be the outward normal on the surface of the solid and let $\mathbf{n}'$ be a unit vector along an arbitrary direction. The presented area of the convex solid in the direction $\mathbf{n}'$ is given by the integral

$$A_p = \int_{\mathbf{n}\cdot\mathbf{n}'>0} \mathbf{n}\cdot\mathbf{n}'\, dS, \tag{A-1}$$

where dS is an element of surface area. The *mean* presented area, averaged over all directions $\mathbf{n}'$, is given by

$$\bar{A}_p = \frac{1}{4\pi}\int d\Omega' \int_{\mathbf{n}\cdot\mathbf{n}'>0} \mathbf{n}\cdot\mathbf{n}'\, dS, \tag{A-2}$$

where the first integral is over all solid angles of a unit sphere. Interchanging the order of integration, we have

$$\bar{A}_p = \int dS \frac{1}{4\pi} \int_{\mathbf{n}\cdot\mathbf{n}'>0} \mathbf{n}\cdot\mathbf{n}'\, d\Omega'. \tag{A-3}$$

In the last integral, $\mathbf{n}$ remains fixed while $\mathbf{n}'$ varies over all solid angles such that $\mathbf{n}\cdot\mathbf{n}' > 0$. By changing coordinates so that $\mathbf{n}$ is along the polar axis, $\mathbf{n}\cdot\mathbf{n}' = \cos\theta$, and this integral is easily evaluated:

$$\int_{\mathbf{n}\cdot\mathbf{n}'>0} \mathbf{n}\cdot\mathbf{n}'\, d\Omega' = \int_0^{2\pi} d\phi \int_0^{\pi/2} \cos\theta \sin\theta d\theta = \pi. \tag{A-4}$$

Substituting this result into equation (A-3) gives

$$\bar{A}_p = \frac{1}{4}\int dS. \tag{A-5}$$

The integral is the total surface area of the solid, so we have the general result:†

> The mean presented area of a convex solid is one-fourth of the total surface area.

It is a well-known fact that a sphere is the shape that minimizes surface area. With the aid of the above result, we can conclude that the minimum mean presented area of *any* convex solid is

$$\bar{A}_p \geq \frac{1}{4}(\text{surface area of a sphere}) = \pi r^2, \tag{A-6}$$

where r is the sphere radius. Substituting this into the equation $\bar{A}_p = \bar{\gamma}(m/\rho)^{2/3}$, we find that the average shape factor for any convex solid obeys the inequality

$$\bar{\gamma} \geq (3/2)^{2/3}(\pi/4)^{1/3} \approx 1.20899.$$

Notice, in particular, that a right circular cylinder obeys this inequality since it has a minimum average shape factor of $(3/2)(\pi/4)^{1/3} \approx 1.38395$.

† This theorem has been attributed to Cauchy. It was first brought to the author's attention by Dr. Robert Shnidman who also outlined this particular derivation.

INTENTIONALLY LEFT BLANK.

APPENDIX B:
SHAPE FACTOR OF A SPIN-STABLIZED FRAGMENT SIMULATOR

The dimensions of the chisel-nose fragment simulator[1] are shown in Figure B-1.

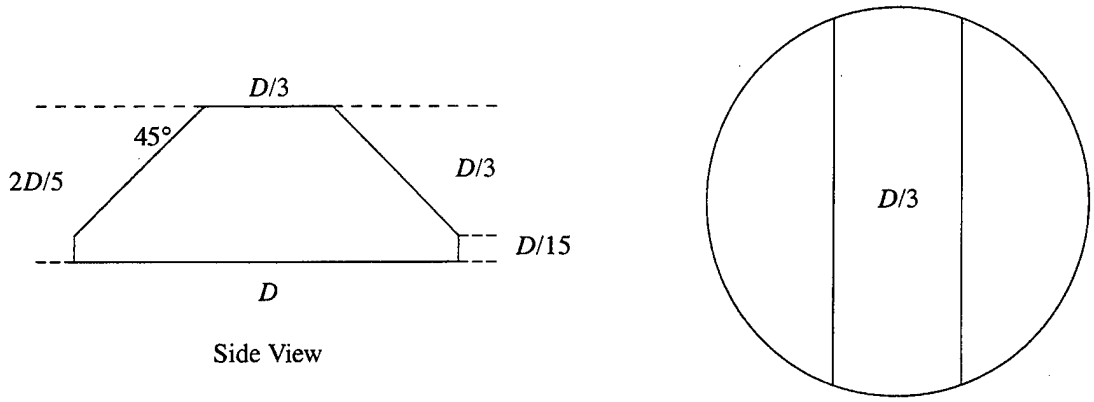

Figure B-1. Dimensions of Fragment Simulator.

Shape Factor

The fragment is spin-stablized so that the chisel nose is forward. The dimensionless shape factor, γ, is defined by

$$A_p \equiv \gamma(m/\rho)^{2/3}, \tag{B-1}$$

where

A_p is fragment presented area (cm^2),
m is fragment mass (gm), and
ρ is fragment density (gm/cm^3).

Volume

The fragment volume, m/ρ, can be calculated as follows:

Total Volume = Volume of Cylinder with Diameter D and Height $2D/5$ – Volume of Chiseled Edges. (B-2)

The volume of the chiseled edges can be calculated using the coordinate system shown in Figure B-2.

1 Fisher, Todd J. and Robert Shnidman. "An Empirical Model for Predicting Electrical Cable Failures in Modern Combat Vehicles," ARL-MR-28, U.S. Army Research Laboratory, Aberdeen Proving Ground, MD, January 1993.

$$x^2 + (y + \frac{D}{6})^2 = \frac{D^2}{4}$$

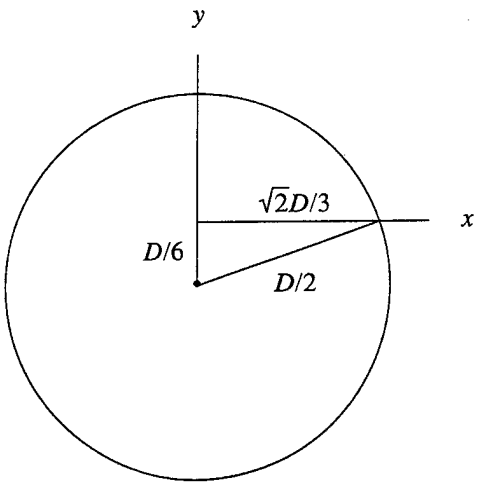

Figure B-2. Coordinate System for Calculating Volume of Chiseled Edges.

$$\frac{m}{\rho} = \frac{\pi}{4} D^2 \frac{2D}{5} - 4 \int_0^{\sqrt{2}D/3} \frac{1}{2} y^2 dx = \frac{\pi}{10} D^3 - 2 \int_0^{\sqrt{2}D/3} \left[\left(\frac{D^2}{4} - x^2 \right)^{1/2} - \frac{D}{6} \right]^2 dx. \tag{B-3}$$

Carrying out the integrations, we find

$$\frac{m}{\rho} = \left[\frac{\pi}{10} - \frac{19\sqrt{2}}{162} + \frac{\sin^{-1}(2\sqrt{2}/3)}{12} \right] D^3. \tag{B-4}$$

Substituting this into equation (B-1), with $A_p = \pi D^2/4$, gives

$$\gamma = \frac{\pi}{4} \left[\frac{\pi}{10} - \frac{19\sqrt{2}}{162} + \frac{\sin^{-1}(2\sqrt{2}/3)}{12} \right]^{-2/3} \approx 1.97448. \tag{B-5}$$

Shape Factor of a Spin-Stablized Right Circular Cylinder

The shape factor of a (flat nose) right circular cylinder that impacts face-on is

$$\gamma = \left(\frac{\pi}{4} \right)^{1/3} \left(\frac{L}{D} \right)^{-2/3}. \tag{B-6}$$

Thus, the proper L/D ratio to effect a given shape factor γ, is

$$L/D = \sqrt{\pi/4}\, \gamma^{-3/2}. \tag{B-7}$$

NO. OF COPIES	ORGANIZATION
2	DEFENSE TECHNICAL INFORMATION CENTER DTIC DDA 8725 JOHN J KINGMAN RD STE 0944 FT BELVOIR VA 22060-6218
1	HQDA DAMO FDT 400 ARMY PENTAGON WASHINGTON DC 20310-0460
1	OSD OUSD(A&T)/ODDDR&E(R) R J TREW THE PENTAGON WASHINGTON DC 20301-7100
1	DPTY CG FOR RDA US ARMY MATERIEL CMD AMCRDA 5001 EISENHOWER AVE ALEXANDRIA VA 22333-0001
1	INST FOR ADVNCD TCHNLGY THE UNIV OF TEXAS AT AUSTIN PO BOX 202797 AUSTIN TX 78720-2797
1	DARPA B KASPAR 3701 N FAIRFAX DR ARLINGTON VA 22203-1714
1	NAVAL SURFACE WARFARE CTR CODE B07 J PENNELLA 17320 DAHLGREN RD BLDG 1470 RM 1101 DAHLGREN VA 22448-5100
1	US MILITARY ACADEMY MATH SCI CTR OF EXCELLENCE DEPT OF MATHEMATICAL SCI MADN MATH THAYER HALL WEST POINT NY 10996-1786

NO. OF COPIES	ORGANIZATION
1	DIRECTOR US ARMY RESEARCH LAB AMSRL D D R SMITH 2800 POWDER MILL RD ADELPHI MD 20783-1197
1	DIRECTOR US ARMY RESEARCH LAB AMSRL DD 2800 POWDER MILL RD ADELPHI MD 20783-1197
1	DIRECTOR US ARMY RESEARCH LAB AMSRL CS AS (RECORDS MGMT) 2800 POWDER MILL RD ADELPHI MD 20783-1145
3	DIRECTOR US ARMY RESEARCH LAB AMSRL CI LL 2800 POWDER MILL RD ADELPHI MD 20783-1145
	ABERDEEN PROVING GROUND
4	DIR USARL AMSRL CI LP (BLDG 305)

NO. OF COPIES	ORGANIZATION
1	OASD C3I MR BUCHHEISTER RM 3D174 6000 DEFENSE PENTAGON WASHINGTON DC 20310-6000
1	OUSD AT STRT TAC SYS DR SCHNEITER RM 3E130 3090 DEFENSE PENTAGON WASHINGTON DC 20310-3090
1	OUSD AT S&T AIR WARFARE RM 3E139 M MUTZELBUG 3090 DEFENSE PENTAGON WASHINGTON DC 20310-3090
1	OUSD AT S&T LAND WARFARE RM EB1060 A VIILU 3090 DEFENSE PENTAGON WASHINGTON DC 20310-3090
1	UNDER SEC OF THE ARMY DUSA OR ROOM 2E660 102 ARMY PENTAGON WASHINGTON DC 20310-0102
1	ASST SECY ARMY ACQUISITION LOGISTICS TCHNLGY SARD ZD ROOM 2E673 103 ARMY PENTAGON WASHINGTON DC 20310-0103
1	ASST SECY ARMY ACQUISITION LOGISTICS TCHNLGY SARD ZP ROOM 2E661 103 ARMY PENTAGON WASHINGTON DC 20310-0103
1	ASST SECY ARMY ACQUISITION LOGISTICS TCHNLGY SARD ZS ROOM 3E448 103 ARMY PENTAGON WASHINGTON DC 20310-0103

NO. OF COPIES	ORGANIZATION
1	US ARMY MATERIEL CMD DEP CHF OF STAFF FOR RDA SCIENCE TECH ENG AMCRDA T R PRICE 5001 EISENHOWER AVE ALEXANDRIA VA 22333-0001
1	US ARMY RESEARCH LAB AMSRL SL PLANS AND PGMS MGR WSMR NM 88002-5513
1	US ARMY RESEARCH LAB AMSRL SL EA R FLORES WSMR NM 88002-5513
1	US ARMY RESEARCH LAB AMSRL SL EM J PALOMO WSMR NM 88002-5513

NO. OF COPIES	ORGANIZATION
	ABERDEEN PROVING GROUND
1	ARMY TEST EVAL COM AMSTE TM S APG MD 21005-5055
2	US ARMY RESEARCH LAB AMSRL SL DR WADE J BEILFUSS
5	US ARMY RESEARCH LAB AMSRL SL B MS SMITH J FRANZ R SANDMEYER M VOGEL W WINNER
1	US ARMY RESEARCH LAB AMSRL SL BA M RITONDO
1	US ARMY RESEARCH LAB AMSRL SL BD J MORRISSEY
1	US ARMY RESEARCH LAB AMSRL SL BE D BELY
1	US ARMY RESEARCH LAB AMSRL SL BG A YOUNG
1	US ARMY RESEARCH LAB AMSRL SL BN D FARENWALD
1	US ARMY RESEARCH LAB AMSRL SL E M STARKS
1	US ARMY RESEARCH LAB AMSRL SL EM J FEENEY APG EA MD 21010-5423

NO. OF COPIES	ORGANIZATION
5	COMMANDER NAVAL SURFACE WARFARE CTR DAHLGREN DIVISION D DICKINSON CODE G24 D JENNINGS CODE G24 S HOCK CODE G24 T WASMUND CODE G24 G WILLIAMS CODE G202 17320 DAHLGREN RD DAHLGREN VA 22448-5100
1	OSD DOT&E LFT J O BRYON RM 1C730 1700 DEFENSE PENTAGON WASHINGTON DC 20301-1700
2	APPLIED RESEARCH ASSOC INC J YATTEAU R ZERNOW 5941 S MIDDLEFIELD RD SUITE 100 LITTLETON CO 80123
2	APPLIED RESEARCH ASSOC INC J ABELL M BURDESHAW 219 W BEL AIR AVE SUITE 5 ABERDEEN MD 21001
1	DIRECTOR JTCG AS CENTRAL OFC CRYSTAL SQUARE #2 SUITE 1003 1725 JEFFERSON DAVIS HGWY ARLINGTON VA 22202-4102
2	AFRL MNA R WEBB R HUNT 101 EGLIN BVLD SUIRE 302 EGLIN AFB FL 32542-6810
2	46 OG OGML (CHICKEN LITTLE) R STOVALL B THORN 104 CHEROKEE AVE EGLIN AFB FL 32542-5600
2	AAC ENMA K MCARDLE C HOLLAND 101 W EGLIN BLVD SUITE 384 EGLIN AFB FL 32542-5499

NO. OF COPIES	ORGANIZATION
1	COMMANDER US ARMY AMCOM AMSAM RD PS WF L CRAFT REDSTONE ARSENAL AL 35898
1	ASC ENMM H GRIFFIS BLDG 11A 2275 D STREET SUITE 10 WRIGHT PATTERSON AFB OH 45433
1	AFRL VACS M LENTZ BLDG 63 1901 TENTH ST WRIGHT PATTERSON AFB OH 45433
1	AFRL VACS SURVIAC BLDG 45 2130 EIGHTH ST SUITE 1 WRIGHT PATTERSON AFB OH 45433
3	NAVAIRWARCENWPNDIV D HALL D SAITZ R RANDOLPH 1 ADMINISTRATION CIRCLE CHINA LAKE CA 93555-6001
2	SURVICE ENGINEERING D VAN DUSEN K BOWMAN 1003 OLD PHILADELPHIA RD SUITE 3 J FOULK ABERDEEN MD 21001
1	INSTITUTE FOR DEFENSE ANALYSES B TURNER 1801 N BEAUREGARD ST ALEXANDRIA VA 22311-1772
1	UNIV OF ALABAMA IN HUNTSVILLE G ROMANCZUK 301 SPARKMAN DR RI E47 HUNTSVILLE AL 35899

NO. OF COPIES	ORGANIZATION
	ABERDEEN PROVING GROUND
1	ARMY TEST EVAL COM AMSTE TA APG MD 21005-5055
1	US ARMY EVAL ANALYSIS CTR CSTE EAC 4120 SUSQUEHANNA AVE APG MD 21005-3013
1	US ARMY EVAL ANALYSIS CTR CSTE EAC SV 4120 SUSQUEHANNA AVE APG MD 21005-3013
1	DIR USAEAC CSTE EAC APG MD 21005
2	DIR USAMSAA AMXSY J E ATZINGER B PARIS APG MD 21005-5071

NO. OF COPIES	ORGANIZATION
45	DIR USARL AMSRL WM TA M BURKINS J DEHN AMSRL WM TB R FREY P BAKER AMSRL WM TC L MAGNESS W WALTERS AMSRL WM TD D DIETRICH T FARRAND K FRANK M RAFTENBERG S SEGLETES AMSRL SL B J FRANZ M VOGEL AMSRL SL BA E DAVISSON R DIBELKA S JUARASCIO D LYNCH L ROACH AMSRL SL BE R BOWERS R KINSLER T KLOPCIC D NEADES R SANDMEYER R SAUCIER (5 CPS) R SHNIDMAN P TANENBAUM AMSRL SL BD W BAKER J COLLINS R GROTE P MERGLER L MOSS J POLESNE R PRATHER P SWOBODA AMSRL SL BG L LOSIE W MERMAGEN K MURRAY T MUEHL J ROBERTSON AMSRL SL BN (E-3331) E FIORAVANTE B RUTH

INTENTIONALLY LEFT BLANK.

REPORT DOCUMENTATION PAGE

Form Approved
OMB No. 0704-0188

1. AGENCY USE ONLY *(Leave blank)*	2. REPORT DATE	3. REPORT TYPE AND DATES COVERED
	July 2000	Final, Jul 99–Sep 99

4. TITLE AND SUBTITLE
Shape Factor of a Randomly Oriented Cylinder

5. FUNDING NUMBERS
622618AH80

6. AUTHOR(S)
Richard Saucier

7. PERFORMING ORGANIZATION NAME(S) AND ADDRESS(ES)
U.S. Army Research Laboratory
ATTN: AMSRL-SL-BE
Aberdeen Proving Ground, MD 21005-5068

8. PERFORMING ORGANIZATION REPORT NUMBER
ARL-TR-2269

9. SPONSORING/MONITORING AGENCY NAMES(S) AND ADDRESS(ES)

10.SPONSORING/MONITORING AGENCY REPORT NUMBER

11. SUPPLEMENTARY NOTES

12a. DISTRIBUTION/AVAILABILITY STATEMENT
Approved for public release; distribution is unlimited.

12b. DISTRIBUTION CODE

13. ABSTRACT *(Maximum 200 words)*

This report defines a dimensionless shape factor, which is useful for characterizing the penetration potential of projectiles and irregular shaped fragments. The shape factor, so defined, is purely a function of shape and orientation and is independent of mass and material density. The shape factor of some simple shapes is calculated exactly, but the focus of this report is on a right circular cylinder (RCC). Not only is it possible to express the shape factor as a function of the length-to-diameter (L/D) ratio and orientation, but it is also possible to derive an exact, closed-form expression for the shape factor probability distribution. It is found that the probability density function is not a symmetrical distribution about its mode, but rather is highly skewed. This points out the inadequacy of an average shape factor and also carries implications for designing fragment simulating projectiles (FSPs). Furthermore, it is shown that randomly oriented cylinders have potential for simulating behind-armor debris fragments.

14. SUBJECT TERMS	15. NUMBER OF PAGES
shaped factor, presented area, fragments, cylinder, random orientation, behind-armor debris, FSP, L/D, RCC	33
	16. PRICE CODE

17. SECURITY CLASSIFICATION OF REPORT	18. SECURITY CLASSIFICATION OF THIS PAGE	19. SECURITY CLASSIFICATION OF ABSTRACT	20. LIMITATION OF ABSTRACT
UNCLASSIFIED	UNCLASSIFIED	UNCLASSIFIED	UL

INTENTIONALLY LEFT BLANK.

USER EVALUATION SHEET/CHANGE OF ADDRESS

This Laboratory undertakes a continuing effort to improve the quality of the reports it publishes. Your comments/answers to the items/questions below will aid us in our efforts.

1. ARL Report Number/Author ARL-TR-2269 (Saucier) Date of Report July 2000

2. Date Report Received _____

3. Does this report satisfy a need? (Comment on purpose, related project, or other area of interest for which the report will be used.) _____

4. Specifically, how is the report being used? (Information source, design data, procedure, source of ideas, etc.) _____

5. Has the information in this report led to any quantitative savings as far as man-hours or dollars saved, operating costs avoided, or efficiencies achieved, etc? If so, please elaborate. _____

6. General Comments. What do you think should be changed to improve future reports? (Indicate changes to organization, technical content, format, etc.) _____

CURRENT ADDRESS

_____
Organization

_____
Name E-mail Name

_____
Street or P.O. Box No.

_____
City, State, Zip Code

7. If indicating a Change of Address or Address Correction, please provide the Current or Correct address above and the Old or Incorrect address below.

OLD ADDRESS

_____
Organization

_____
Name

_____
Street or P.O. Box No.

_____
City, State, Zip Code

(Remove this sheet, fold as indicated, tape closed, and mail.)
(DO NOT STAPLE)

DEPARTMENT OF THE ARMY

OFFICIAL BUSINESS

NO POSTAGE
NECESSARY
IF MAILED
IN THE
UNITED STATES

BUSINESS REPLY MAIL
FIRST CLASS PERMIT NO 0001,APG,MD

POSTAGE WILL BE PAID BY ADDRESSEE

DIRECTOR
US ARMY RESEARCH LABORATORY
ATTN AMSRL SL BE
ABERDEEN PROVING GROUND MD 21005-5068